Biomaterials Translational

Fabrication, microstructure and properties of advanced ceramic-reinforced composites for dental implants: a review

Mugilan Thanigachalam[*,#], *Aezhisai Vallavi Muthusamy Subramanian*[#]

Key Words:
ceramic composites; flexural strength; fracture toughness; implant materials; sintering; Vickers hardness

From the Contents

ABSTRACT

The growing field of dental implant research and development has emerged to rectify the problems associated with human dental health issues. Bio-ceramics are widely used in the medical field, particularly in dental implants, ortho implants, and medical and surgical tools. Various materials have been used in those applications to overcome the limitations and problems associated with their performance and its impact on dental implants. In this article we review and describe the fabrication methods employed for ceramic composites, the microstructure analyses used to identify significant effects on fracture behaviour, and various methods of enhancing mechanical properties. Further, the collective data show that the sintering technique improves the density, hardness, fracture toughness, and flexural strength of alumina- and zirconia-based composites compared with other methods. Future research aspects and suggestions are discussed systematically.

Department of Mechanical Engineering, Government College of Technology, Coimbatore, Tamil Nadu, India

***Corresponding author:**
Mugilan Thanigachalam, mugilangct@gmail.com.

#Author equally.

http://doi.org/10.12336/biomatertransl.2023.03.004

How to cite this article:
Thanigachalam, M.; Subramanian, A. V. M. Fabrication, microstructure and properties of advanced ceramic-reinforced composites for dental implants: a review. *Biomater Transl.* **2023**, *4*(3), 151-165.

Introduction

Global biomedical research in industry has been driven rapidly due to several limitations of dental implants such as short service life, failure rate, and poor functional performance. Ceramics are non-metallic materials which are made from combinations of metal and non-metallic components. The essential properties of ceramics are high strength, high hardness, excellent oxidation resistance, low thermal conductivity, and good corrosion resistance. However most ceramics are monolithic, and some special engineering functions cannot be achieved effectively due to their brittle nature.[1] Consequently the principal intention for working on ceramic matrix composites (CMCs) is to enhance the current options and increase the many applications in the fields of engineering and medicine.[2, 3] These can be achieved by making modifications to existing composites and then implementing new combinations of matrix and reinforcements.[4]

CMCs have excellent thermal shock resistance, are resistant to wear, possess excellent creep behaviour, and exhibit improved fracture toughness.[5] The causes of crack initiation and development such as material fatigue, over loading, and residual stress in ceramic material have been investigated and many strengthening mechanisms have been employed to avoid the formation of cracks in the tip area using filler materials. High temperatures and thermal shocks are a necessary aspect of various engineering applications. Typically, tubes are present in the flow heat exchangers, cutting tool inserts, and gasoline turbines in automobile industries, particularly aerospace appliances[6] "*The common reinforcements especially applied in dental ceramic composites are titanium carbide (TiC), carbon nanotubes (CNTs), titanium nitride (TiN), boron nitride (BN), carbon nanofibres (CNF), carbon powder, graphene, etc.*" Spark plasma sintering (SPS) and hot pressing are the most common and effective techniques for preparing composites with higher temperature ranges. In addition to the temperature limitation, other limitations of this method include degradation. Another limitation of CMCs is that they cannot be used to make complex shapes. During sintering of CMCs

also leads to thermal stress introduction. So conventional or non-conventional machining (NCM) processes are used when additional manufacturing steps are necessary. The known methods used for machining ceramics and their composite are drilling and grinding. Both these methods are tricky for complex shape and require more time to machine and machining the complex shape.[7] "*Ultrasonic machining (USM), abrasive jet machining (AJM), abrasive water jet machining (AWJM), laser machining, and electric discharged machining (EDM) are the important cost reduction techniques in modern CNC*".[8] NCM processes can reduce the cost and gear up by eliminating or reducing the need for secondary machining. Also, most NCM techniques reduce the requirement for costly cutting tools, because material is removed by erosion and abrasion with a simple primary source. Mechanical abrasion, melting or evaporation, chemical dissolution, and electrochemical dissolution are developed machining techniques involved in ceramic machining involving material removal.[9] For the last three decades, remarkable development has been achieved in all kinds of ceramic frames for use in dental restoration applications. Combined aesthetic veneering porcelains for all restorations are made up of ceramics that consist of fluorapatite, leucite, or aluminium oxide as the crystalline phase and glass with high strength ceramic cores, particularly zirconium-oxide or aluminium-oxide, and lithium-disilicate. All ceramics consist of a more significant proportion of different crystalline phases, which differs from metal-ceramics.[10] This is the main reason underlying the improvements in mechanical properties of all ceramics, but more substantial opacity can develop, which is not advisable for ceramics used in dental applications. Various factors can increase or decrease the transparency of a material: the grain size, microstructure particle orientation, phase refractive index, and refractive index.[11] Consequently there is a greater potential to develop a clear, transparent appearance using alumina and zirconia ceramics, and the recent alumina series provides greater translucency by using special materials suitable for clinical use.

Dental ceramic materials are classified based on the ceramic system, transparency, microstructure, fabrication temperature, material composition, and usage. Based on these parameters, the glass-to-crystalline ratio, the geometry of crystalline structure and size, and the mismatch between the crystal thermal expansion, Young's modulus, and phase changes, significantly influence the properties and performance of dental ceramic materials.[12, 13]

To improve the properties of a material, it is generally essential to increase its density through stage adjustment (using another stage of grain development); dynamic sintering (adding another substance to build mass vehicle); responsive sintering (the utilization of added importance to forestall loss of stoichiometry), and through liquid-stage sintering. Consequently, the sintering cycle can be improved by sintering added substances, which are utilized to balance out the desired glasslike structures, or added to the liquid stage to aid increased densification. In this sense, a glassy phase can be a sintering added substance. Indeed, the sintering cycle in the presence of a glass (liquid stage sintering) can happen at a lower temperature in the examination of dry sintering (sintering measure without a polished stage). Liquid stage sintering includes the arrangement of fluids because of the various softening temperatures of the segments. The liquid phase accounts for 1% to 20% of the volume. Control of the microstructure of ceramic materials is critical because it permits acquisition of data to measure the exhibition of these materials in help. In dental ceramic production, surface cracks can be distinguished through the fluorescent penetrant liquid technique or identified through acoustic emission, optically or interferometrically. Also, the various essential factors involved in the design consideration of dental implants are biocompatibility, bio- and osseointegration, biomechanics, corrosion resistance, material compositions, and mechanical properties. Recent dental implant materials, shapes, and factors considered in the design of dental implants are shown in **Figure 1**. In this article we attempt to review the research dealing with the various fabrication methods, microstructural analysis, and some essential mechanical properties of ceramic composites used in dental implants.

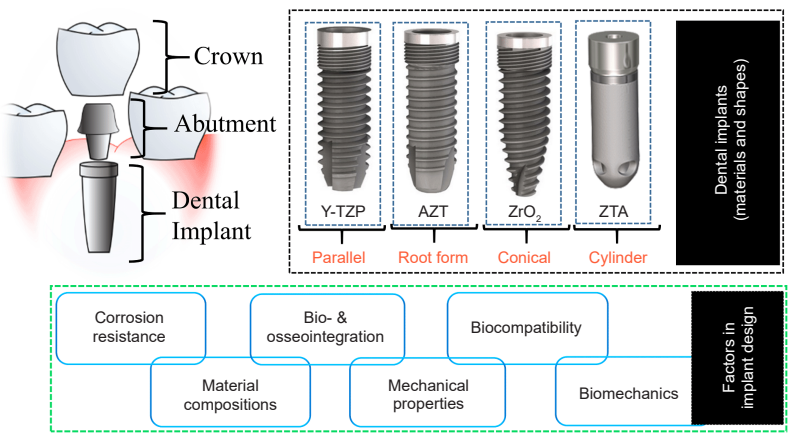

Figure 1. Materials and factors considered in the design of dental implants. AZT: alumina-toughened zirconia; Y-TZP: yttria-stabilised tetragonal zirconia polycrystalline; ZrO_2: zirconium dioxide; ZTA: zirconia-toughened alumina.

Materials and Fabrication Methods Involved in Ceramic Composites

The most significant ceramic materials used in dental implant application are listed. Zirconia (ZrO_2) is known for its excellent biocompatibility and strength, and thus is widely used for dental implant abutments and frameworks. Alumina (Al_2O_3) ceramics offer high strength and wear resistance, making them suitable for dental implant applications. Hydroxyapatite (HA) is a bioactive ceramic often used as a coating on dental implant surfaces to enhance osseointegration. Bioactive glass can bond with bone tissue and can be used in dental implant coatings. Tricalcium phosphate (TCP) ceramics have properties of biocompatibility and resorbability, making them useful in dental implant applications. Yttria-stabilised zirconia (YSZ) ceramics combine the properties of zirconia with enhanced stability due to yttria stabilization. Lithium disilicate is used for making dental crowns and bridges due to its aesthetic properties and strength.[14] Glass-ceramics such as leucite-reinforced ceramics are used in dental restorations due to their natural appearance and strength. Silicon nitride (Si_3N_4) ceramics, although less common, have been investigated for dental implant applications due to their mechanical properties. Calcium phosphate ceramics offer bioactivity and can support bone regeneration around dental implants. The choice of a ceramic material depends on various factors including its mechanical properties, biocompatibility, aesthetics, and intended application within the dental implant system.[15]

Titanium and its alloys are widely used for dental implants due to their biocompatibility. Researchers are focusing on developing innovative surface modifications to enhance osseointegration and promote better bone integration. Zirconia continues to be popular for dental implants, and researchers are exploring ways to improve its properties further by blending it with other materials or modifying its microstructure. Biodegradable materials, such as magnesium alloys or polymers, are being studied for use as temporary implants and as scaffolds for tissue regeneration. These materials gradually degrade over time as new tissue forms.

Researchers are working on developing advanced ceramic composites with improved mechanical properties and aesthetics for dental implant applications. One such material is polyether ether ketone (PEEK)-based biopolymers reinforced by different ceramic particulates like titanium dioxide (TiO_2) and silicon dioxide (SiO_2) with surface modifications. These modifications provide improved mechanical strength and excellent osteointegration.[16-19]

Various coatings and bioactive agents are being investigated to improve implant-bone bonding, prevent infections, and stimulate tissue regeneration. Smart implants are implants embedded with sensors or electronics that are being explored for real-time monitoring of implant conditions, healing progress, and potential issues.

Based on functional requirements, properties, and application, CMCs can be fabricated by various techniques as described by multiple investigators: dry pressing (uniaxial compacting), hot isostatic compacting, and cold isostatic compacting of powder ceramics.[20] The major important factors adopted for the fabrication of CMCs are operating temperature, type of reinforcement used, and the size and shape of the composites required, which depend on an application basis.[21] The liquid phase process contains the sol-gel and polymer infiltration pyrolysis processing methods. Slip casting and powder metallurgy are the most applicable techniques for preparing composites in the solid phase.[22] Because these techniques can be applied to ceramic materials with high melting points, like titanium, zirconium, tungsten, molybdenum, and tantalum, they can also achieve homogenous particle distribution. These can reduce the need for subsequent machining and increase the powder-to-product percentage. The gas-phase process includes reaction bonding, chemical vapour deposition, and chemical vapour infiltration. Reinforcement and matrix phase produce the chemical reaction that has controlled conditions in the gas phase reaction, and these techniques include reaction bonding and chemical vapour infiltration processes. Much recent research undertaken to reduce the processing temperature and time are using powder metallurgical techniques to achieve a high rate of densification, to produce a near net shape, and the energy requirement is less for growth and nucleation properties.[23]

Compressive strength and bulk density are the critical properties of CMCs in many applications. Still, there is some disadvantage to achieving these properties in reaction bonding of materials in the sintering technique with a temperature range from 1450°C to 1700°C. The single microwave cavity method has also been used to obtain a pore-free and homogeneous composite instead of sintering.[24] The weight percentage and fracture toughness of the preceramic polymer polycarbosilane can be increased. The material's porosity can be decreased in preceramic polymer reaction bonding by fabricating porous ceramics. The phase-wise fabrication techniques are classified into liquid, solid, and gas phases, illustrated in **Figure 2**. The commercially-available dental zirconia systems are tabulated in **Table 1**.[25] Most implant manufacturing companies moved towards one-piece type implants with various shapes such as conical, cylindrical, and root forms because the process and material properties are critically important in two-piece type implants.

Melting infiltration in the reaction bonding technique has been adopted for manufacture of silicon carbide (SiC)/CNT composite. The proper distribution of reinforcement is assured by using this technique, leading to better electrical conductivity properties. By increasing the graphite content, the open porosity of the multi-bonded porous ceramic increases, and it can be decreased by improving the temperature and forming pressure of the sintering process. Due to gaseous oxidation within products, open pores are formed.[26] There is an improvement in flexure strength with increased multiplication which is achieved by increasing sintering temperature. The reaction bonding process protects the oxidation of SiC with formation of a gel intermediary.[27] At the various temperatures of the ferro molybdenum (FeMO) alloy fabrication process, the effect of alloying confers excellent physical properties on CMCs.[28] A similar study has been carried out in the reaction-bonded technique of silicon nitride by adding lithium oxide

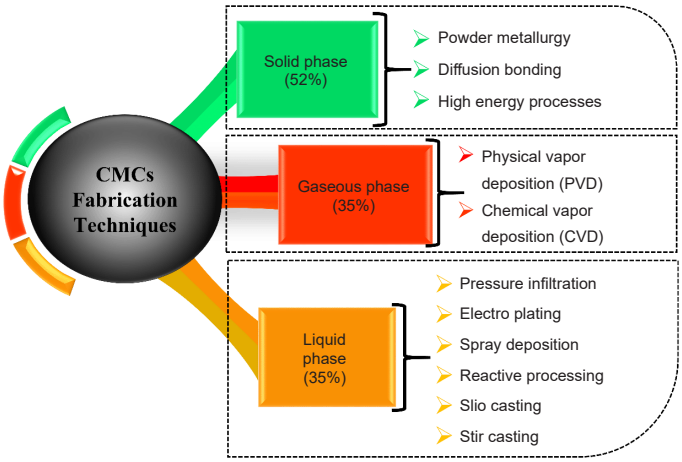

Figure 2. Ceramic matrix composite fabrication processes. CMCs: ceramic matrix composites; CVD: chemical vapour deposition; PVD: physical vapour deposition.

Table 1. Implant manufacturers and zirconia implant materials

Implant material	Product name	Manufacturer
Alumina-toughened zirconia	ZERAMEX (P)lus	Dental point AG, Spreitenbach, Switzerland
	FairWhite™	Fair implant, Schleswig-Holstein, Germany
	SDS – Swiss Dental Solutions 1.0 DT	SDS Swiss Dental Solutions AG, Kreuzlingen, Switzerland
Yttria-stabilised tetragonal zirconia polycrystalline	CeraRoot	CeraRoot S.L, Barcelona, Spain
	Ceralog	Camlog System, Basel, Switzerland
	SDS 2.2	SDS AG, Kreuzlingen, Switzerland
	ICX-White	MKI GmbH &Co.KG, Stuttgart, Germany
	REPLICATE™ System	Natural Dental Implant AG, Berlin, Germany
Zirconia oxide	Konus K3Pro ZirKon Implant system	Argon Medical Productions, Plano, TX, USA
	Easy Kon	General Implants, Wurmlingen, Germany
	Whitesky	Bredent medical, Senden, Germany
	CeraRoot	
	(S)andard ZV3	ZV3-ZirconVison GmbH, Munchen, Germany
	Ceramic implant	VITA Zahnfabrik, Wurttemberg, Germany

(LiO_2) and Si powder. The findings revealed that regardless of Al impurity, when there is a decrease in thermal conductivity, the purity of Si powder increases, and the presence of LiO_2 also increases. The effective way of determining the bending strength of a composite is the four-point bending method. In this case, Si powder with course level addition gives the best result of about 700 MPa and 11 MPa·$m^{1/2}$ of fracture toughness.[29] The addition of various sizes of particles to reaction-bonded boron carbide gives excellent fracture toughness. The presence of pores in reaction-bonded boron carbide ceramic due to residual silicon affects the fracture toughness property. Where there is a decrease in volume fraction, the hardness of reaction-bonded boron carbide composite increases because it contains larger-sized particles.[30] Decreasing the residual silicon quality of the composite will give a reduction in porosity. By using nano-sized zirconia powder, the SiC growth will increase, a method of composite fabrication which provides an increased level of flexural strength and fracture toughness.

The densification rate has been increased and the temperature reduced for vanadium pentoxide (V_2O_5). The effect of reinforcement by addition of SiC particles in the nitration gives higher density and achieves the required mechanical properties and explicit microstructure.[31] The addition of 10% SiC particles in the sintered specimen gives better mechanical properties of reaction bonding between the silicon nitrate composites.[32] The two-step freeze casting technique has been implemented for composite fabrication to reduce thermal reaction in SiC ceramics, creating an overall shape with improved strength. Material deposition is associated with various ceramics, metal alloys, and semiconductors with coatings of thin and thick layers. An advanced method such as thermal plasma chemical vapour deposition produces enhanced results compared to the other conventional deposition methods. The SiC/Si_3N_4 alpha-beta phase is formed in a controlled manner. The gas turbine materials, semiconducting material, various coatings of ceramic composites, and fibre-reinforced composites are

broad application areas in the CVD and sintering processes. During the sintering process, the particles of ceramic and reinforcement are compressed after the compacting process using a gravity die setup at high temperatures. A grain boundary will develop due to the hot pressing between the particles. This forms a connective structure with the help of neck formation. A higher compressive force and the effect of higher temperature maintain the neck growth formation which tends to develop and become densified. During this process, the porosity of the ceramic composite is reduced due to the temperature effect on the densification process. Pore-free ceramic structures are being fabricated using sintering techniques.[33] Densification through neck formation in the sintering process is shown in **Figure 3**.

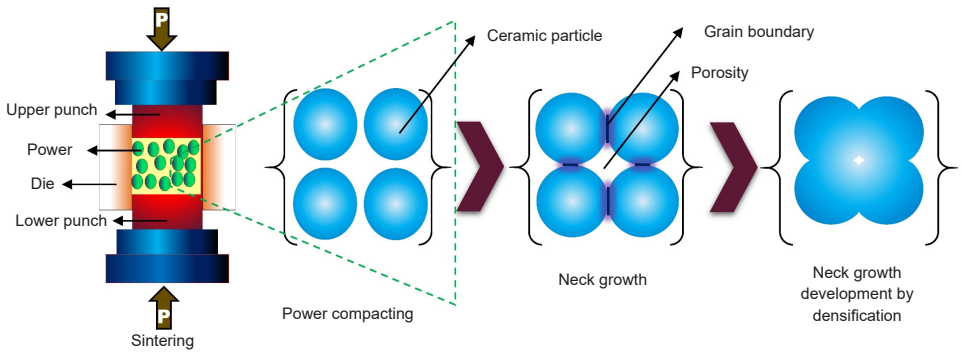

Figure 3. Grain growth development by densification.

The fabrication techniques suitable for ceramic composites based on their crystalline structure are listed in **Figure 4**. **Figure 5** shows the sintering techniques divided into general categories. Based on pressure-assisted and pressureless sintering, the state, the type of phases that the material possesses, and stress level, whether it is considered high-stress or low-stress level, have been classified. In phase-oriented classification, processes are further divided into liquid and solid phases under which sub-entities are included for consideration while selecting the type of sintering. The actual sintering process stages are classified into three stages, starting from the heating stage, holding for a particular temperature and finally cooling the specimen. During the first stage of this process, the temperature of the tip increases because of the gradual increment of tip displacement. Sintering is a critical step in the fabrication process of dental implants, particularly when using ceramics or metal alloys. Sintering involves heating the implant components at elevated temperatures but below their melting points. This process leads to the fusion of particles, resulting in densification, increased mechanical strength, and improved material properties. Sintering is essential to achieve the required structural integrity and biocompatibility of dental implant materials, ensuring that the implant materials are strong enough to withstand the mechanical forces exerted during chewing and other oral functions. Additionally, sintering helps achieve a biocompatible surface that allows for proper osseointegration, which is the fusion of the implant with the surrounding bone. The specifics of sintering, such as temperature, atmosphere, and time, depend on the material being used. Dental implant manufacturers carefully optimise these parameters to achieve the desired structural and biocompatible properties required for successful dental implantation. In **Table 2**, the grain size and sintering parameters and their relationship to relative density are shown.[34]

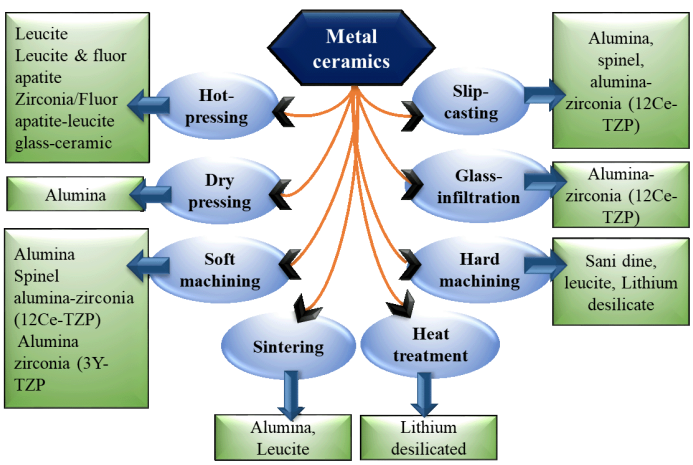

Figure 4. Appropriate fabrication techniques for various crystalline phases. 12Ce-TZP: 12 ceria stabilized tetragonal zirconia polycrystals; 3Y-TZP: 3 yttriastabilised tetragonal zirconia polycrystalline.

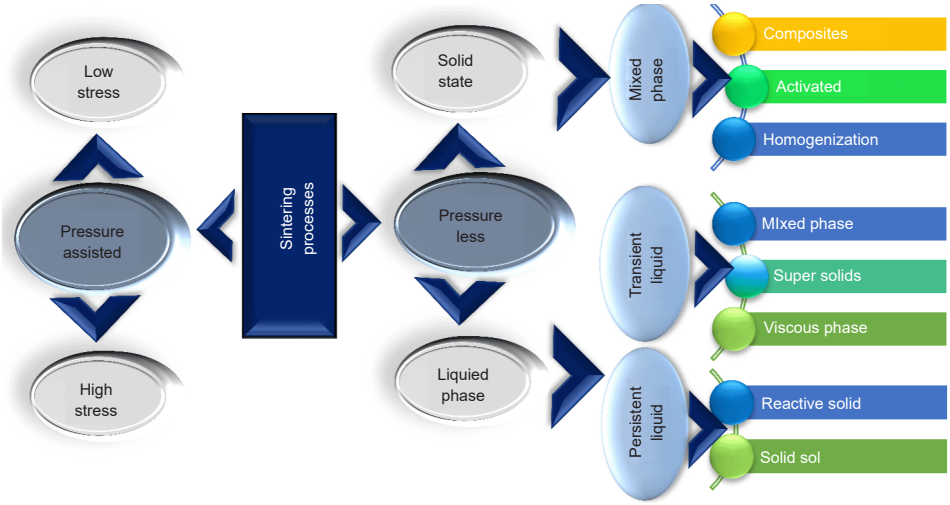

Figure 5. Classification of sintering processes.

Table 2. Summary of the sintering process of alumina-toughened zirconia

Sintering method	Sintering temperature (°C)	Holding time (minutes)	Relative density (%)	Grain size (nm)		Codes[a]
				Zirconia	Alumina	
Microwave sintering (MW)	1200	10	98.5	210±64	270±84	MW120010
	1200	30	99	240±67	300±100	MW120030
	1300	10	99.8	280±75	400±157	MW130010
	1300	30	99.8	280±70	380±146	MW130030
Conventional sintering (CS)	1400	120	98.3	240±41	350±98	CS1400120
	1500	120	99.2	330±56	450±100	CS1500120

Note: [a]First two letters indicate the method of sintering, next four digits indicates sintering temperature in degrees Celsius and last two digits indicate holding time in minutes.

Microstructure Studies

Microstructure analyses of dental ceramic composites were performed to improve understanding of the distribution of particles and elements, the presence of grains, phases, and molecular structure. This type of analysis is also used to study the surface characteristics of prepared composites. The surface characterisation includes surface morphology, fracture, fatigue, and grain growth analyses on the surface. The various microstructure examination techniques carried out were scanning electron microscopy (SEM), field emission SEM, and transmission electron microscopy using standard fracture and fatigue tested specimens for comparison. All dental ceramic composite such as ZrO_2, Al_2O_3, aluminium titanate (Al_2TiO_5), TiO_2, chromic oxide (Cr_2O_3), alumina-toughened zirconia (ATZ), and ZTA have various kinds of microstructural behaviour associated with their composition. Consequently, the addition of reinforcement gives an enhanced microstructure suitable for a particular application. The addition of reinforced particles such as oxides provides a densified microstructure. If the presence of Ni content increases within the structure, ceramic composites will give better densities than specimens with smaller pore sizes.[35] Usually, these gradual additions give the specimen a better relative density, due to the uniform spreading of nickel particles, which has been clearly shown in microstructure images. The authors suggested that the process of sintering is well suited to generating a material with a highly dense grain structure.[36]

The ceramic material tools used in the dental implant fabrication process consist of a very dense and refined microstructure of graphene particles with different contents. Improved strength has been achieved due to the mature dispersal of graphene particles in the CMCs, especially given the excellent distribution of various size grains. Less fractured surfaces were detected in SEM images of these graphite tool materials with tungsten carbide (WC).[37] An extensive fracture was determined at about 68% in the notch region of 2Ce-TZP compared to the monoclinic phase 3Y-TZP. Also, there was no micro-cracked zone in 3Y-TZP.[38] This analysis also revealed exciting facts about the various regions of the fracture surface specimens: from the initial notch crack to the final fracture. It was concluded that R curves help predict the stress intensity factor concerning crack length. The fracture surface of TSP with various crack regions is shown in **Figure 6**.

In the 3Y-TZP/Ta ceramic composite, the pressure applied perpendicular or parallel to the orientation of an SPS specimen was observed in SEM images. The Ta particles in the TZP composites give the material fracture toughness up to 15 $MPa{\cdot}m^{1/2}$. These microstructure images show the partial debonding of the Ta particles during plastic deformation due to

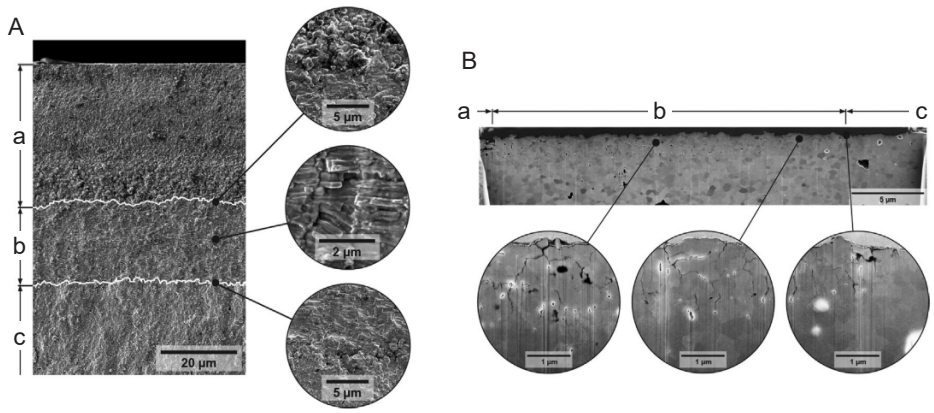

Figure 6. (A) Fracture surface, where three different regions are distinguished: notch (a), micro-cracked area (b), and regular fracture surface (c). (B) The cross-sectional view obtained by focused ion beam analysis of the fracture surface. Reprinted from Turon-Vinas and Anglada.[38] Copyright 2018 The Academy of Dental Materials.

the toughening process. The presence of Ta particles increases the crack growth resistance.[39] The focusing wavelength range of the SEM images also gives a better understanding of the various phenomena in the particle addition or any mechanism involved in improving the properties in this investigation. The 3LM type SEM with an EDX chemical microanalyzer was used for microstructural characterisation to identify the presence of phases. Crack propagation will occur because of the flake-shaped particles used in the SPS process with the applied pressure with uniform dispersion and proper orientation. Pressure-less rapid sintering of Al_2O_3 and ZrO_2 with various range compositions reveals the dense structure of the particles in SEM images with a constant sintering temperature of 1550°C per 2-minute duration and heating rates of 5°C to 100°C per minute.[40] The restriction of the densification process in the dental ceramic comprises a ZrO_2-Al_2O_3 base, purely based on the effect of zirconia.

SEM graphs of ZrO_2 (partially stabilized zirconia, PSZ) composites give the proper distribution of the particles and greater electron density brightens the zirconium (Zr) presence region. The particles did not possess the particular effect of base-pinned grain boundaries of alumina. Calcium magnesium-based ceramics have granular crystal morphology that includes microfracture because of grain size and distribution. If grain size is below 10 µm, the grain will give better distribution of images. Hot presses ceramic composites have higher density compared to other fabrication technique composites, and the standard atomic ratios of Ca, Mg, and Al are comparatively lower and are tightly bonded during sintering.[41] Nitrogen absorption is an effective analytical method for calculating the primary size of particles.[42] This technique can achieve the best particle dispersion. Alumina carbon composite created by sintering at 1400°C produces highly porous ceramics. This porosity was measured by the water absorption method. The technique of field emission gun-scanning electron microstructure is used for this analysis. Fracture morphologies of porous Si_3N_4-Si_3N_4 with 30 µm scale and different deposition times in hours reveal that the fracture of the porous structure is high.[43] Fracture morphologies of porous Si_3N_4-Si_3N_4 with various deposition times at 30 µm magnification are shown in **Figure** 7. SEM images of the fracture surfaces of Zr-based composites are shown in **Figure 8**.

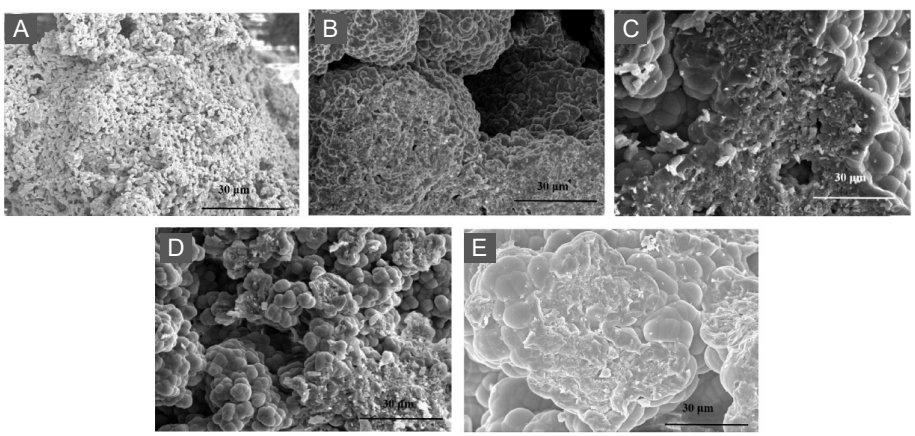

Figure 7. Fracture morphologies of porous Si_3N_4–Si_3N_4 composite ceramics as a function of deposition time: (A) 0, (B) 3, (C) 6, (D) 9, and (E) 12 hours. Scale bars: 30 µm. Si_3N_4: silicon nitride. Reprinted from Cheng et al.[43]

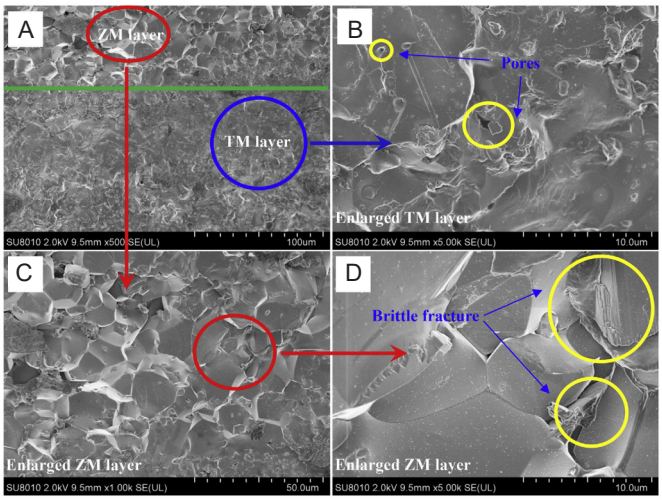

Figure 8. Scanning electron microscopic images of fracture surfaces. Scale bars: 100 μm (A), 10 μm (B, D), 50 μm (C). Reprinted from Liu et al.[4] Copyright 2019 Elsevier Ltd and Techna Group S.r.l.

Mechanical Properties

General properties of ceramic materials include high melting point, high hardness strength, physical properties those hinder the performance, high modulus of elasticity, good chemical resistance, and low malleability. Normally ceramic composite materials have been proven to be ionic materials so valence is warranted. These materials may be crystalline in structure or amorphous in nature. The substandard or enhanced mechanical properties lead to fracture and various deformations.[44] To overcome the brittle nature, ceramic material has been incorporated into the different reinforcement categories. Crack formation also developed as a result of the poor mechanical properties of ceramics. These limitations can be resolved by improving the mechanism of mechanical property improvement.

Vickers hardness

One factor influencing the hardness of the material is grain size; another is relative density. These two factors have been suggested to significantly affect the hardness of ATZ composites in most material research concerning a particular fabrication technique called sintering.[45] In the Vickers hardness test, monolithic ceramic composites like Al_2O_3-TiN increased 65% and achieved 24.6 GPa. A Vickers diamond pyramid-type indenter is a micro-indentation primarily suitable for prediction of dental bilayer structure hardness. Nanoindentation type hardness computation of standard specimens prepared on ceramics decreases slightly with Ni content addition. The effect of graphene on the hardness of ceramic tools has been improved up to 24.64 GPa.

Meanwhile, the hardness decreased due to the destruction of the microstructure. Hardness values of 1700 Vickers hardness number (VHN) have been achieved in many ATZ ceramic composites. The Zr toughened alumina ceramics reached 1120 VHN. The Y-TZP, tetragonal grain-based ceramics, have a 1200-VHN value. The hardness value of ceria-stabilised zirconia-based composites is 1160 VHN. The case of PSZ with alumina has a VHN of 16.31 MPa, a 30% improvement due to the addition of yttrium doping. The titanium (Ti) and graphene flakes significantly affect the ceramic hardness resulting in a 25% improvement. Due to the high sintering temperature of approximately 1650°C, under 35 MPa pressure, 20.1 GPa VHN has been achieved. The Vickers hardness value of Ti alumina-based ceramic has reached 37 GPa due to the increase of Ti particles in the alumina. Most sintering processes have been performed only after particle grain size reduction. The effect that increasing the sintering temperature on Vickers hardness has on variation in alumina ceramics with yttria-partially stabilised zirconia (Y-PSZ) is shown in **Figure 9**. Sintering temperature plays a vital role in obtaining the hardness and elastic modulus of alumina and zirconia-based ceramic composites.[46] The effect of sintering temperature on Vickers hardness and elastic modulus at the addition of zirconia is shown in **Figure 10**.

Decreasing the grain size results in a densified composite so that the hardness value increases because of the improvement in indentation resistance properties of the composites.[47] The ZrB_2–SiC–Ni with ball-milled sintering produces a composite hardness value of up to 20.2 GPa VHN. The two essential models of Vickers hardness prediction are the proportional specimen resistance[48] model using Meyer law and the Tabor model based on the theory of rigid material indentation related to yield stress. Using these kinds of empirical models, the indentation load-size effect of a material can be calculated. In Meyer law, it gives the relational existence between applied load (P) and indentation size (a), as shown in equation (1),

$$P = Ha^n \quad (1)$$

Where n is the Meyer index, and H is the constant. The specimen resistance can be calculated by using the following equation (2) according to Hays and Kendall,[46]

$$R = p_1 a \quad (2)$$

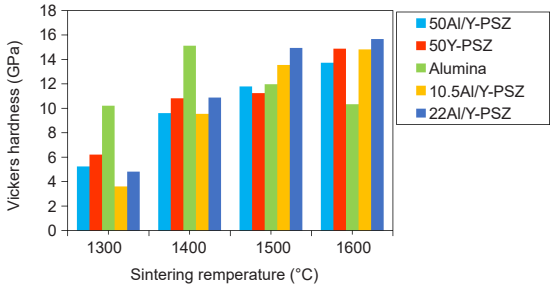

Figure 9. Effect of sintering temperature on Vickers hardness of alumina ceramics.

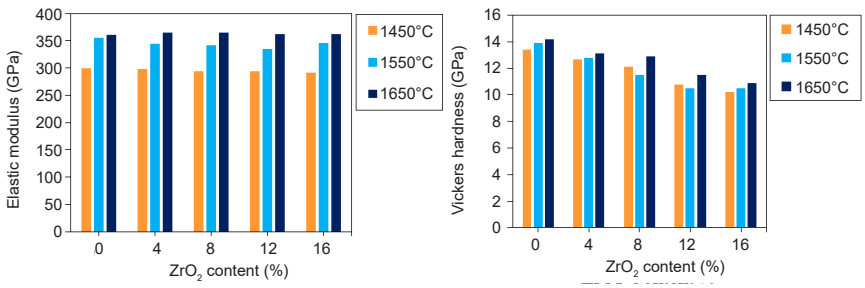

Figure 10. Effect of zirconia addition on elastic modulus and Vickers hardness at various sintering temperatures. ZrO_2: zirconium dioxide.

After that, effective indentation load and dimensions for indentation are relatively calculated by using the following equation (3),

$$P_{effective} = P - R = P - p_1 a = p_2 a^2 \quad (3)$$

Some modified versions of proportional specimen resistance models can be helpful for the determination of indentation hardness at the surface caused by induced residual stresses that occur while machining the specimen. Equation (4) depicts the relationship between the indentation parameters and indentation size,

$$P = \alpha + p_1 a + p_2 a^2 \quad (4)$$

Where α is the constant, and p_1 and p_2 are the proportional specimen resistance model parameters. These kinds of semi-empirical models are also beneficial to determining the nano level of the VHN of the ceramic materials, which have crystalline and monolithic forms, by using the following equation (5),

$$VHN = 1.8544 \frac{P_{effective}}{a^2} \quad (5)$$

The micro-Vickers hardness number of non-strain hardening specimens can be calculated by using the Tabor relation, which is related to yield stress yield σ_{yield} and load in equation (6),

$$VHN = 2.9\sigma_{yield} \quad (6)$$

Using this equation, the effects of indentation of the coated surface of ceramic composites can be calculated.

Fracture toughness

Fracture toughness is an important mechanical property for dental implant materials because this implies the reliability of products. The toughness value of most AZT ceramics is about 4.0 MPa·m$^{1/2}$ to 5.0 MPa·m$^{1/2}$ due to the high zirconia content. Zirconia-based ceramics have moderate fracture toughness values up to 4.5 MPa·m$^{1/2}$. Due to the tetragonal grains in the Y-TZP, fracture toughness increases from about 8.0 MPa·m$^{1/2}$ to 10.0 MPa·m$^{1/2}$, which is the highest value compared to the other types of dental ceramics.[49] The fracture toughness (FT) of microwave-sintered specimens were comparatively much better than those of other densified specimens prepared by conventional sintering. The peak value of fracture toughness achieved was 6.3 MPa·m$^{1/2}$ with microwave sintering (MS)130010 and the lowest was 4.9 MPa·m$^{1/2}$ with conventional sintering (CS) 1400120. Usually, the fracture toughness value increases with the increase of sintering temperature due to ceramic particle bonding. Also, higher sintering temperatures produce enhanced densities,[50, 51] so fracture toughness can reach exceptionally high values with SPS. In non-conventional techniques, the fracture toughness value improvement is highly possible with ZrB_2-SiC-Ni-ultra high temperature ceramics which achieve comparatively excellent toughness only because of their Ni content. The toughness value reaches a mean of 8.3 MPa·m$^{1/2}$ in ZrB_2-SiC ceramics. The reason for this improvement is that increasing the Ni content confers appropriate modifications in the macro defect reduction, due to the thermal expansion coefficient of the ceramic particles.[52] The toughness value is changed for the following reasons: one is the mis-match of the values, and another is the external load. So usually, low fracture toughness ceramics have limited practical applications.[53]

Figure 11 shows the fracture-toughening mechanism of zirconia composites. Initially, the zirconia particles in the monoclinic phase reach the crack initiation stage. Then, the phase-changing phenomenon transforms the monoclinic phase zirconia particles into tetragonal phase zirconia. Crack propagation is controlled by tetragonal phase zirconia due to its formation of covalent solid bonds after the phase-changing process. The technical analysis of surface cracks influenced by fracture toughness was carried out in alumina-based ceramics using crack length measurement. Based on that analysis, the crack initiation mechanism was formulated and then identically analysed and controlled in high-purity alumina ceramics. The standard empirical models used in direct crack length measurements are the Anstis and Palmqvist crack analysis models.[54] The effect of zirconia on fracture toughness at various grain sizes is shown in **Figure 12**. Initiating nucleation on a specific grain located on the surface triggers a process leading to the formation of micro-cracks and exerting stress on neighbouring regions within the transformed zone. This, in turn, results in extensive micro-cracking and a roughened surface. The orange pathway illustrates the penetration that occurs due to micro-cracking encircling the transformed grains. To overcome the limited resilience of alumina as well as the susceptibility of zirconia to ageing, the current trend involves the creation of alumina-zirconia composites. This approach offers the potential to harness the advantages of zirconia's toughness-enhancing mechanism while circumventing the significant drawback associated with its transformation when exposed to steam or bodily fluids. A recent review of literature about alumina-zirconia composites developed for biomedical applications reveals a range of compositions, spanning from zirconia-rich to alumina-rich, that have been subjected to testing.[55]

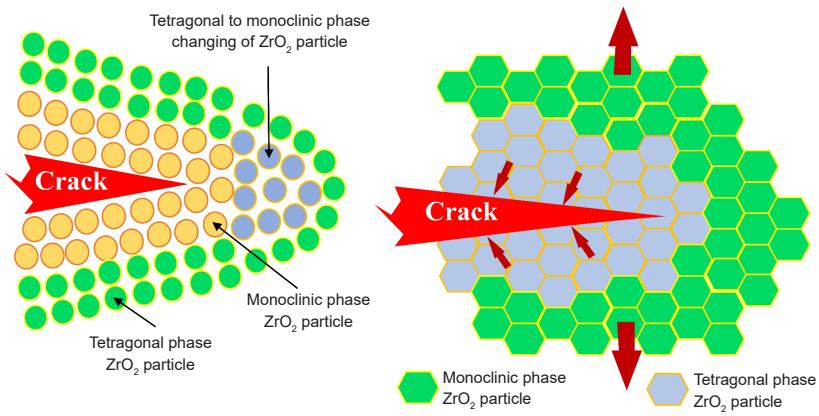

Figure 11. Toughening mechanism in zirconia against crack propagation. ZrO_2: zirconium dioxide.

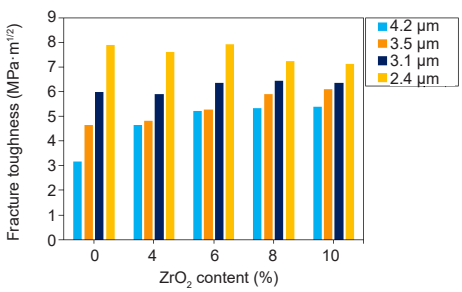

Figure 12. Effect of ZrO_2 content on fracture toughness at various grain sizes. ZrO_2: zirconium dioxide.

Ceramic materials used in dental implants and other structural applications primarily involve a transformation toughening process. Zirconia undergoes a crystallographic phase transformation when subjected to certain stress conditions, which imparts enhanced toughness and resistance to crack propagation. This transformation toughening mechanism is key to improving the overall mechanical reliability of zirconia ceramics.

Tetragonal to monoclinic transformation works as follows, zirconia exists in several crystallographic phases, with the most relevant ones for dental applications being tetragonal and monoclinic phases. Under normal conditions, zirconia is stabilised in its tetragonal phase due to the addition of stabilizing elements like yttria (Y_2O_3) during the manufacturing process. By harnessing this transformation toughening mechanism, zirconia ceramics can exhibit improved fracture toughness and resistance to crack propagation. This property is highly beneficial in dental implant materials, where the prevention of cracks and the ability to withstand chewing forces are critical for long-term performance and durability.[56]

Flexural strength

Flexural strength is increased by the addition of increasing amounts of Ti and Mg ceramic particles. This strength has improved up to 625 MPa in a single direction. The addition of graphene reinforcement to the zirconia will give a 30% improvement in flexural strength value of 590 MPa, mainly in monolithic zirconia. If the material is very dense, meaning it achieves better flexural strength, then due to the density, the strength increases up to 47 MPa. In the case of ATZ, the composite has produced a range of flexural strength between 450–700 MPa due to the greater content of zirconia.[57] At the same time, 604 MPa is also predicted in the ZTA.[58] Here also, grain size plays a significant role in improving implant strength. Thus, minimizing the grain size will help achieve a higher range of strength. The tetragonal grains give tremendous strength values to dental implant materials; the range is 1000 MPa to 1300 MPa. Ceria-stabilised zirconia gives the highest flexural strength value at 1500 MPa. From this, monolithic zirconia is only suitable for particular strength basis applications, so combinations of zirconia and other oxides give higher flexural strength. The effect of TiO_2 content on flexural strength for various sintering temperatures gives better flexural strength at a 5% addition of TiO_2 with all sintering temperatures.[59] **Figure 13** shows the effect of ZrO_2 content on flexural strength at various sintering temperatures. The mechanical properties of the zirconia implant materials are shown in **Figure 14**. The systematically-collected literature of materials, methods, and results of analysis of mechanical properties for ceramic composites from various research papers in recent years are listed in **Table 3**. *In-vitro* testing involves subjecting dental implant materials to controlled laboratory conditions. Flexural strength testing measures the material's ability to withstand bending or flexing forces. This is typically done using a three-point or four-point bending test setup. Higher flexural strength indicates better resistance to bending and potential for withstanding occlusal forces in the oral environment. The most common method for determining fracture toughness is using the single-edge notched beam test or compact tension test. Higher fracture toughness values indicate a greater ability to resist crack initiation and propagation, which is essential for preventing implant failure due to stress concentration and fatigue.[17]

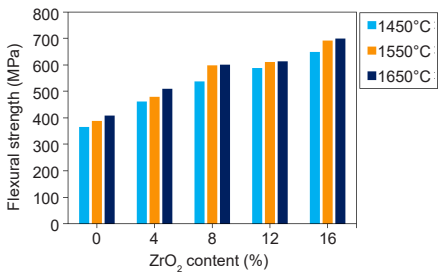

Figure 13. Effect of ZrO_2 content on flexural strength at various sintering temperatures. ZrO_2: zirconium dioxide.

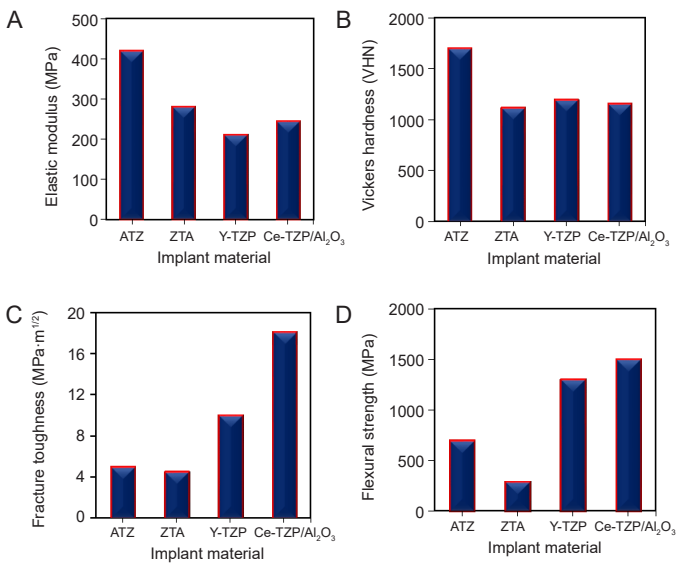

Figure 14. Mechanical properties of different implant materials. (A) Elastic modulus. (B) Vickers hardness. (C) Fracture toughness. (D) Flexural strength. Al_2O_3: aluminium dioxide; AZT: alumina toughened zirconia; TPZ: tetragonal phase zirconia; Y-TZP: Yttria-stabilised tetragonal zirconia polycrystalline; ZTA: zirconia toughened alumina.

Table 3. Systematic literature collection of results from recent research

Studies	Ceramic composites	Method of mixing	Conditions for sintering	Results
Liu et al.[4]	Al_2O_3–ZrB_2–MgO/ Al_2O_3–TiN–MgO	Planetary ball milling machine, alumina ball to powder ratio 1:3	Hot pressed, vacuum at 1650°C, 60 minutes under 35 MPa.	Flexural strength = 654 ± 43 MPa, fracture toughness = 8.7 ± 0.2 MPa·$m^{1/2}$, Vickers hardness = 20.1 ± 0.5 GPa, elastic modulus = 351 GPa
Tovar-Vargas et al.[59]	Yttrium doped ZrO_2–Al_2O_3 composite powders with partially stabilised ZrO_2 (PSZ)	Wet ball milling	Pressing (370 MPa); Sintering (1600°C/5 hours)	Highest Kc ~8.40 ± 0.4 MPa and hardness ~16.31 ± 0.58 GPa were obtained for the 30 wt% PSZ-Al_2O_3
Smirnov et al.[21]	Hierarchical tantalum-graphene flakes reinforced zirconia	Ball milling	Spark plasma sintering (maximum temperatures of 1400 and 1500°C under vacuum at a heating rate of 100°C/min, and applied pressure of 80 MPa)	Flexural strength 30% increment and toughness 175% increase compared to monolithic Zr
Liu et al.[60]	ρ-Al_2O_3	Wet-milled with a rotating speed of 300 r/min for 3 hours	Compacted at 10 MPa, sintered at a heating rate of 5°C/min to 1600°C, 3 hours	Hot modulus of rupture = 6.26 MPa, thermal shock resistance = 2.53
Yan et al.[36]	ZrB_2–SiC–Ni	Ball-milled for 12 hours	Spark plasma sintering	Fracture toughness = 8.3 MPa,
Smirnov et al.[39]	3Y-TZP/Ta	High-energy ball milling	spark plasma sintering, vacuum (≈ 1×10^2 Mbar) at 1400°C, 200°C/min	Flexural strength = 967 MPa, surface roughness Ra = 0.3 ± 0.1
Prajzler et al.[40]	Alumina based zirconia ceramics	Ball milling	Pressureless rapid rate sintering (100°C/min to 1500°C/min)	Nearly total density (> 95% TD) without forming cracks or other structural defects.
Ke et al.[41]	WcoB-TiC	Planetary ball milling machine	Sintering at 1500°C, 60 minutes	Hardness = 91.6 HRA, transverse rapture strength = 1783 MPa.
Cheng et al.[43]	Porous Si_3N_4–Si_3N_4	Ball milling	Sintering and 3D printing combined with low-pressure chemical vapour infiltration	Density increased from 0.99 to 2.02 g/cm^3 flexural strength of 47 ± 2 MPa
Manshor et al.[61]	TiO_2 (ZTA–TiO_2) Cr_2O_3	Ball milling	Sintering 1600°C for 1 hour with 5°C/min	Fracture toughness increased to 7.15 MPa·$m^{1/2}$ by adding up to 0.6 wt% Cr_2O_3
Zhu et al.[62]	$MgTiO_3$/CaO-B_2O_3-SiO_2	Ball milling with ethyl alcohol for 300 minutes	Sintered at 810°C, 120 minutes	Bulk density = 3.1270 g/cm^3, flexural strength = 214.85 MPa
Wang et al.[63]	Al_2O_3/TiC	Hybrid slurries form ball-milling for 60 hours	Hot-pressing sintering 1700–1750°C in a nitrogen atmosphere, 35 MPa	Fracture toughness = 97 MPa·$m^{1/2}$, Vickers hardness = 37 GPa
Zhang et al.[64]	SiAlON–Si_3N_4	Ball milling	Reaction-bonded sintering, 4°C/min to 1500°C	Compressive strength = 185 MPa
Zhao et al.[65]	ZrB_2–SiC–Ni	Ball-milled for 12 hours using ZrO_2 ball media	Spark plasma sintering, 1400°C for 1 minute, 200°C/min	Hardness = 20.2 GPa, elastic modulus of ZS =53.7 GPa
Li et al.[66]	CM_2A_8 ($CaMg_2Al_{16}O_{27}$) and $C_2M_2A_{14}$ ($Ca_2Mg_2Al_{28}O_{46}$)	Calcinated at 900°C for 1 hour	Hot press sintering 1750°C, 15 MPa.	Vickers hardness = 12.95 GPa, fracture toughness = 2.17 MPa, flexural strength = 248 MPa

Note: 3D: three-dimensional; Al_2O_3: aluminium dioxide; B_2O_3: boron trioxide; $C_2M_2A_{14}$: stable calcium aluminate phase; CaO: calcium oxide; CM_2A_8: ternary stable calcium aluminate phase; Cr_2O_3: chromic oxide; Kc: fracture toughness; MgO: magnesium oxide; $MgTiO_3$: magnesium titanium oxide; Si_3N_4: silicon nitride; SiAlON: formation of silicon nitride, aluminium oxide and aluminium nitride; SiC: silicon carbide; SiO_2: silicon dioxide; TD: total density; TiC: titanium carbide; TiN: titanium nitride; TiO_2: titanium dioxide; WCoB: tungsten cobalt boron; Y-TZP: yttria-stabilised tetragonal zirconia polycrystalline; ZrB_2: zirconium diboride; ZrO_2: zirconium dioxide; ZS: zirconium diboride with silicon carbide; ZTA: zirconia-toughened alumina.

Ex-vitro analysis involves assessing dental implant materials in real-world clinical settings, such as in patients' mouths. This includes monitoring patients over an extended period to evaluate the long-term performance of the implants. Clinical studies provide valuable information on how implants perform under actual oral conditions, considering factors like occlusal forces, oral hygiene, and patient habits.[18]

Conclusion and Future Scope

The current scenario of zirconia ceramics in dental applications has been providing expected mechanical properties and biological integration enhancement in the material world.

• The application of zirconia-based CMCs can be an excellent alternative to titanium-based implants because of the rapid developments in the medical field. In the last decade, the

application of dental zirconia and alumina-based ceramics has improved.

• Implant fabrication in conventional methods has manifested some limitations, so there is a need to improve densified composites that advanced sintering techniques can achieve. Computer-aided design-oriented 3D manufacturing techniques also provide a suitable route to achieve near net shape without material waste.

• Mechanical perspective comes with clinical research aspects that keep on searching for materials to replace titanium implants. Most researchers focus on AZT and ZTA alone, without any combination, mainly bio oxides.

• The future focus of dental implant material with biocompatible oxides helps to further enhance the performance of the implant, such as resistance to minor fracture, strength, and functionality. The different combinations of zirconia implants can be a promising alternative that is looking to refine mechanical competencies. Collaboration of clinical dentistry research with *in-vitro* and *in-vivo* studies of enhanced bioceramic composites and material processing technologies is required for rapid development in bioceramic research.

Dental implant technology is continually evolving, and review papers may become outdated relatively quickly. New materials, techniques, and research findings may emerge after this review has been published. Review papers often focus on a specific aspect of dental ceramic implants or a subset of relevant studies. This limited scope may not cover all available research or provide a comprehensive overview of the field.

Author contributions

MT: Conceptualization, data curation, writing - original draft, writing - review & editing; AVMS: supervision, review & editing. Both authors reviewed and approved the final version of the manuscript.

Financial support

None.

Acknowledgement

The first author would like to give his sincere thanks to Dr. M.S. Aezhisai Vallavi for their immense support and valuable suggestions.

Conflicts of interest statement

The authors declare that they have no conflict of interest.

1. Wójcik, N. A.; Tagiara, N. S.; Möncke, D.; Kamitsos, E. I.; Ali, S.; Ryl, J.; Barczyński, R. J. Mechanism of hopping conduction in Be–Fe–Al–Te–O semiconducting glasses and glass–ceramics. *J Mater Sci.* **2022**, *57*, 1633-1647.
2. Magnani, G.; Fabbri, P.; Leoni, E.; Salernitano, E.; Mazzanti, F. New perspectives on zirconia composites as biomaterials. *J Compos Sci.* **2021**, *5*, 244.
3. Taeh, A. S.; Othman, F. M.; Abdul-Hamead, A. A. Reviewing alumina-zirconia composite as a ceramic biomaterial. *Hunan Daxue Xuebao.* **2022**, *49*, 263-273.
4. Liu, C.; Sun, J.; Li, G.; Li, B.; Gong, F. Fabrication, mechanical properties and fracture behaviors of the laminated Al_2O_3–ZrB_2–MgO / Al_2O_3–TiN–MgO ceramic composite. *Ceram Int.* **2020**, *46*, 857-865.
5. Williams, T.; Yeomans, J.; Smith, P.; Heaton, A.; Hampson, C. Effect of interfacial area on densification and microstructural evolution in silicon carbide–boron carbide particulate composites. *J Mater Sci.* **2016**, *51*, 353-361.
6. Alcudia-Ramos, M. A.; Fuentez-Torres, M. O.; Ortiz-Chi, F.; Espinosa-González, C. G.; Hernández-Como, N.; García-Zaleta, D. S.; Kesarla, M. K.; Torres-Torres, J. G.; Collins-Martínez, V.; Godavarthi, S. Fabrication of g-C_3N_4/TiO_2 heterojunction composite for enhanced photocatalytic hydrogen production. *Ceram Int.* **2020**, *46*, 38-45.
7. Pradhan, S.; Singh, S.; Prakash, C.; Królczyk, G.; Pramanik, A.; Pruncu, C. I. Investigation of machining characteristics of hard-to-machine Ti-6Al-4V-ELI alloy for biomedical applications. *J Mater Res Technol.* **2019**, *8*, 4849-4862.
8. Saeed, F.; Muhammad, N.; Khan, A. S.; Sharif, F.; Rahim, A.; Ahmad, P.; Irfan, M. Prosthodontics dental materials: From conventional to unconventional. *Mater Sci Eng C Mater Biol Appl.* **2020**, *106*, 110167.
9. Lin, C.; Zhao, Q.; Zhao, X.; Yang, Y. Cavitation erosion of metallic materials. *Int J Georesources Environment.* **2018**, *4*, 1-8.
10. Ramachandran, K.; Boopalan, V.; Bear, J. C.; Subramani, R. Multi-walled carbon nanotubes (MWCNTs)-reinforced ceramic nanocomposites for aerospace applications: a review. *J Mater Sci.* **2022**, *57*, 3923-3953.
11. Meena, K. L.; Vidyasagar, C. S.; Benny Karunakar, D. Mechanical and tribological properties of MgO/multiwalled carbon nanotube-reinforced zirconia-toughened alumina composites developed through spark plasma sintering and microwave sintering. *J Mater Eng Perform.* **2022**, *31*, 682-696.
12. Condi Mainardi, J.; Bonini Demarchi, C.; Mirdrikvand, M.; Karim, M. N.; Dreher, W.; Rezwan, K.; Maas, M. 3D bioprinting of hydrogel/ceramic composites with hierarchical porosity. *J Mater Sci.* **2022**, *57*, 3662-3677.
13. Bartoli, M.; Duraccio, D.; Faga, M. G.; Piatti, E.; Torsello, D.; Ghigo, G.; Malucelli, G. Mechanical, electrical, thermal and tribological behavior of epoxy resin composites reinforced with waste hemp-derived carbon fibers. *J Mater Sci.* **2022**, *57*, 14861-14876.
14. Osman, R. B.; Swain, M. V. A critical review of dental implant materials with an emphasis on titanium versus zirconia. *Materials (Basel).* **2015**, *8*, 932-958.
15. Tartsch, J.; Blatz, M. B. Ceramic dental implants: an overview of materials, characteristics, and application concepts. *Compend Contin Educ Dent.* **2022**, *43*, 482-488; quiz 489.
16. Thanigachalam, M.; Muthusamy Subramanian, A. V. Evaluation of PEEK-TiO(2)- SiO(2) nanocomposite as biomedical implants with regard to in-vitro biocompatibility and material characterization. *J Biomater Sci Polym Ed.* **2022**, *33*, 727-746.
17. Muthusamy Subramanian, A. V.; Thanigachalam, M. Mechanical performances, in-vitro antibacterial study and bone stress prediction of ceramic particulates filled polyether ether ketone nanocomposites for medical applications. *J Polym Res.* **2022**, *29*, 318.
18. Thanigachalam, M.; Muthusamy Subramanian, A. V. In-vitro cytotoxicity assessment and cell adhesion study of functionalized nTiO2 reinforced PEEK biocompatible polymer composite. *Polym Plasts Technol Mater.* **2022**, *61*, 566-576.
19. Mugilan, T.; Aezhisai Vallavi, M. S.; Sugumar, D. Materialistic characterization, thermal properties, and cytocompatibility investigations on acrylic acid-functionalized nSiO2-reinforced PEEK polymeric nanocomposite. *Colloid Polym Sci.* **2022**, *300*, 1155-1168.
20. Zhai, X.; Zhang, X.; Ma, Y.; Liu, J. Influence of Bi_2O_3, TiO_2 additives

and sintering process on the performance of ITO target based on normal pressure sintering method. *Trans Indian Ceramic Soc.* **2019**, *78*, 83-88.

21. Smirnov, A.; Peretyagin, P.; Bartolomé, J. F. Processing and mechanical properties of new hierarchical metal-graphene flakes reinforced ceramic matrix composites. *J Eur Ceram Soc.* **2019**, *39*, 3491-3497.
22. Qian, K.; Yao, Z.; Lin, H.; Zhou, J.; Haidry, A. A.; Qi, T.; Chen, W.; Guo, X. The influence of Nd substitution in Ni–Zn ferrites for the improved microwave absorption properties. *Ceram Int.* **2020**, *46*, 227-235.
23. Ghosh, R.; Sarkar, R. Comparative analysis of novel calcium phosphate based machinable bioceramic composites. *Trans Indian Ceramic Soc.* **2020**, *79*, 131-138.
24. Raghavendra, C. R.; Basavarajappa, S.; Sogalad, I.; Naik, K. Study on wear mechanism and contact temperature against dry sliding wear of Ni-Al2O3 nanocomposite coating. *Trans Indian Ceramic Soc.* **2020**, *79*, 139-143.
25. Yadav, P.; Rattan, S.; Tripathi, A.; Kumar, S. Tailoring of complex permittivity, permeability, and microwave-absorbing properties of CoFe2O4/NG/PMMA nanocomposites through swift heavy ions irradiation. *Ceram Int.* **2020**, *46*, 317-324.
26. Liu, C.; Li, X.; Wu, Y.; Zhang, L.; Chang, X.; Yuan, X.; Wang, X. Fabrication of multilayer porous structured TiO_2–$ZrTiO_4$–SiO_2 heterostructure towards enhanced photo-degradation activities. *Ceram Int.* **2020**, *46*, 476-486.
27. Avcıoğlu, S.; Buldu, M.; Kaya, F.; Üstündağ, C. B.; Kam, E.; Menceloğlu, Y. Z.; Kaptan, H. Y.; Kaya, C. Processing and properties of boron carbide (B_4C) reinforced LDPE composites for radiation shielding. *Ceram Int.* **2020**, *46*, 343-352.
28. Zhang, H.; Li, M.; Zhu, C.; Tang, Q.; Kang, P.; Cao, J. Preparation of magnetic α-Fe_2O_3/$ZnFe_2O_4$@Ti_3C_2 MXene with excellent photocatalytic performance. *Ceram Int.* **2020**, *46*, 81-88.
29. Zhang, Z.; Lin, T.; Shao, H.; Peng, J.; Wang, A.; Zhang, Y.; Yu, X.; Liu, S.; Wang, L.; Zhao, M. Effect of different dopants on porous calcium silicate composite bone scaffolds by 3D gel-printing. *Ceram Int.* **2020**, *46*, 325-330.
30. Song, S.; Gao, Z.; Lu, B.; Bao, C.; Zheng, B.; Wang, L. Performance optimization of complicated structural SiC/Si composite ceramics prepared by selective laser sintering. *Ceram Int.* **2020**, *46*, 568-575.
31. Su, N. K.; Rejab, N. A.; Ahmad, Z. A.; Abdullah, N. S. Densification of zirconia toughened alumina added CeO_2 ceramics via hot isostatic press sintering technique. *Key Eng Mater.* **2022**, *908*, 228-233.
32. Thankachan, T.; Soorya Prakash, K.; Malini, R.; Ramu, S.; Sundararaj, P.; Rajandran, S.; Rammasamy, D.; Jothi, S. Prediction of surface roughness and material removal rate in wire electrical discharge machining on aluminum based alloys/composites using Taguchi coupled Grey Relational Analysis and Artificial Neural Networks. *Appl Surf Sci.* **2019**, *472*, 22-35.
33. Adibpur, F.; Tayebifard, S. A.; Zakeri, M.; Shahedi Asl, M. Spark plasma sintering of quadruplet ZrB_2–SiC–ZrC–Cf composites. *Ceram Int.* **2020**, *46*, 156-164.
34. Gil-Flores, L.; Salvador, M. D.; Penaranda-Foix, F. L.; Dalmau, A.; Fernández, A.; Borrell, A. Tribological and wear behaviour of alumina toughened zirconia nanocomposites obtained by pressureless rapid microwave sintering. *J Mech Behav Biomed Mater.* **2020**, *101*, 103415.
35. Xia, Y.; Mou, J.; Deng, G.; Wan, S.; Tieu, K.; Zhu, H.; Xue, Q. Sintered ZrO_2–TiO_2 ceramic composite and its mechanical appraisal. *Ceram Int.* **2020**, *46*, 775-785.
36. Yan, X.; Jin, X.; Li, P.; Hou, C.; Hao, X.; Li, Z.; Fan, X. Microstructures and mechanical properties of ZrB_2–SiC–Ni ceramic composites prepared by spark plasma sintering. *Ceram Int.* **2019**, *45*, 16707-16712.
37. Cui, E.; Zhao, J.; Wang, X. Determination of microstructure and mechanical properties of graphene reinforced Al_2O_3-Ti(C, N) ceramic composites. *Ceram Int.* **2019**, *45*, 20593-20599.
38. Turon-Vinas, M.; Anglada, M. Strength and fracture toughness of zirconia dental ceramics. *Dent Mater.* **2018**, *34*, 365-375.
39. Smirnov, A.; Peretyagin, P.; Bartolomé, J. F. Wire electrical discharge machining of 3Y-TZP/Ta ceramic-metal composites. *J Alloys Compd.* **2018**, *739*, 62-68.
40. Prajzler, V.; Salamon, D.; Maca, K. Pressure-less rapid rate sintering of pre-sintered alumina and zirconia ceramics. *Ceram Int.* **2018**, *44*, 10840-10846.
41. Ke, D.; Pan, Y.; Wu, R.; Xu, Y.; Wang, P.; Wu, T. Effect of initial Co content on the microstructure, mechanical properties and high-temperature oxidation resistance of WCoB-TiC ceramic composites. *Ceram Int.* **2018**, *44*, 1213-1219.
42. Rakshit, R.; Das, A. K. A review on cutting of industrial ceramic materials. *Precis Eng.* **2019**, *59*, 90-109.
43. Cheng, Z.; Ye, F.; Liu, Y.; Qiao, T.; Li, J.; Qin, H.; Cheng, L.; Zhang, L. Mechanical and dielectric properties of porous and wave-transparent Si_3N_4-Si_3N_4 composite ceramics fabricated by 3D printing combined with chemical vapor infiltration. *J Adv Ceram.* **2019**, *8*, 399-407.
44. Srinivasan, V. P.; Palani, P. K.; Selvarajan, L. Experimental investigation on electrical discharge machining of ceramic composites (Si_3N_4-TiN) using RSM. *Int J Comput Mater Sci Surf Eng.* **2018**, *7*, 104-115.
45. Kuntz, M.; Krüger, R. The effect of microstructure and chromia content on the properties of zirconia toughened alumina. *Ceram Int.* **2018**, *44*, 2011-2020.
46. Monzavi, M.; Zhang, F.; Meille, S.; Douillard, T.; Adrien, J.; Noumbissi, S.; Nowzari, H.; Chevalier, J. Influence of artificial aging on mechanical properties of commercially and non-commercially available zirconia dental implants. *J Mech Behav Biomed Mater.* **2020**, *101*, 103423.
47. Gao, P. Z.; Cheng, L.; Yuan, Z.; Liu, X.-p.; Xiao, H.-n. High temperature mechanical retention characteristics and oxidation behaviors of the $MoSi_2(Cr_5Si_3)$—RSiC composites prepared via a PIP—AAMI combined process. *J Adv Ceram.* **2019**, *8*, 196-208.
48. Machaka, R.; Derry, T. E.; Sigalas, I.; Herrmann, M. Analysis of the Indentation Size Effect in the Microhardness Measurements in B_6O. *Adv Mater Sci Eng.* **2011**, *2011*, 539252.
49. Singaravel Chidambara Nathan, A.; Tah, R.; Balasubramanium, M. K. Evaluation of fracture toughness of zirconia silica nano-fibres reinforced feldespathic ceramic. *J Oral Biol Craniofac Res.* **2018**, *8*, 221-224.
50. Liao, Y.; Wang, Y.; Chen, Z.; Wang, X.; Li, J.; Guo, R.; Liu, C.; Gan, G.; Wang, G.; Li, Y.; Zhang, H. Microstructure and enhanced magnetic properties of low-temperature sintered LiZnTiMn ferrite ceramics with Bi_2O_3-Al_2O_3 additive. *Ceram Int.* **2020**, *46*, 487-492.
51. Talimian, A.; Galusek, D. Aqueous slip casting of translucent magnesium aluminate spinel: Effects of dispersant concentration and solid loading. *Ceram Int.* **2019**, *45*, 10646-10653.
52. Hou, P. J.; Guo, Y. F.; Sun, L. X.; Deng, G. Q. Simulation of temperature and thermal stress filed during reciprocating traveling WEDM of insulating ceramics. *Procedia CIRP.* **2013**, *6*, 410-415.
53. Caravaca, C. F.; Flamant, Q.; Anglada, M.; Gremillard, L.; Chevalier, J. Impact of sandblasting on the mechanical properties and aging

resistance of alumina and zirconia based ceramics. *J Eur Ceram Soc.* **2018**, *38*, 915-925.
54. Jindal, P. C. A new method for evaluating the indentation toughness of hardmetals. *Crystals.* **2018**, *8*, 197.
55. Ahmad, I.; Islam, M.; Al Habis, N.; Parvez, S. Hot-pressed graphene nanoplatelets or/and zirconia reinforced hybrid alumina nanocomposites with improved toughness and mechanical characteristics. *J Mater Sci Technol.* **2020**, *40*, 135-145.
56. Chen, X.; Liu, C.; Zheng, W.; Han, J.; Zhang, L.; Liu, C. High strength silica-based ceramics material for investment casting applications: Effects of adding nanosized alumina coatings. *Ceram Int.* **2020**, *46*, 196-203.
57. Yu, H.; Hou, Z.; Guo, X.; Chen, Y.; Li, J.; Luo, L.; Li, J.; Yang, T. Finite element analysis on flexural strength of Al_2O_3-ZrO_2 composite ceramics with different proportions. *Mater Sci Eng A.* **2018**, *738*, 213-218.
58. Rao, P. K.; Jana, P.; Ahmad, M. I.; Roy, P. K. Synthesis and characterization of zirconia toughened alumina ceramics prepared by co-precipitation method. *Ceram Int.* **2019**, *45*, 16054-16061.
59. Tovar-Vargas, D.; Roitero, E.; Anglada, M.; Jiménez-Piqué, E.; Reveron, H. Mechanical properties of ceria-calcia stabilized zirconia ceramics with alumina additions. *J Eur Ceram Soc.* **2021**, *41*, 5602-5612.
60. Liu, J.; Huo, W.; Zhang, X.; Ren, B.; Li, Y.; Zhang, Z.; Yang, J. Optimal design on the high-temperature mechanical properties of porous alumina ceramics based on fractal dimension analysis. *J Adv Ceram.* **2018**, *7*, 89-98.
61. Manshor, H.; Azhar, A. Z. A.; Rashid, R. A.; Sulaiman, S.; Abdullah, E. C.; Ahmad, Z. A. Effects of Cr_2O_3 addition on the phase, mechanical properties, and microstructure of zirconia-toughened alumina added with TiO_2 (ZTA–TiO_2) ceramic composite. *Int J Refract Met Hard Mater.* **2016**, *61*, 40-45.
62. Zhu, X.; Kong, F.; Ma, X. Sintering behavior and properties of $MgTiO_3$/CaO-B_2O_3-SiO_2 ceramic composites for LTCC applications. *Ceram Int.* **2019**, *45*, 1940-1945.
63. Wang, X.; Zhao, J.; Cui, E.; Song, S.; Liu, H.; Song, W. Microstructure, mechanical properties and toughening mechanisms of graphene reinforced Al_2O_3-WC-TiC composite ceramic tool material. *Ceram Int.* **2019**, *45*, 10321-10329.
64. Zhang, L.; Liu, X.; Li, M.; Xu, E.; Zhao, F.; Yuan, H.; Sun, X.; Zhang, C.; Gao, L.; Gao, J. Feasibility of SiAlON–Si_3N_4 composite ceramic as a potential bone repairing material. *Ceram Int.* **2020**, *46*, 1760-1765.
65. Zhao, H.; Li, Z.; Zhang, M.; Li, J.; Wu, M.; Li, X.; Chen, J.; Xie, M.; Li, J.; Sun, X. High-performance Al_2O_3–YAG:Ce composite ceramic phosphors for miniaturization of high-brightness white light-emitting diodes. *Ceram Int.* **2020**, *46*, 653-662.
66. Li, B.; Li, G.; Chen, H.; Chen, J.; Hou, X.; Li, Y. Physical and mechanical properties of hot-press sintering ternary CM_2A_8 ($CaMg_2Al_{16}O_{27}$) and $C_2M_2A_{14}$ ($Ca_2Mg_2Al_{28}O_{46}$) ceramics. *J Adv Ceram.* **2018**, *7*, 229-236.

Received: June 30, 2023
Revised: August 7, 2023
Accepted: September 8, 2023
Available online: September 28, 2023